IAC-24,A3,IP,192,x87805

Integrated Approach for Water Production and Additive Manufacturing Using Magnetically-Beneficiated Lunar Regolith

Maxim Isachenkov[a], Alice Dottori[b], Ivan Troisi[c*], Antonio Mattia Grande[d], Michèle Lavagna[e], Giuseppe Sala[f]

[a] *PhD student, Politecnico di Milano, Department of Aerospace Science and Technology, Via La Masa, 34, 20156 Milano – Italy*, maxim.isachenkov@polimi.it
[b] *PhD student, Politecnico di Milano, Department of Aerospace Science and Technology, Via La Masa, 34, 20156 Milano – Italy*, alice.dottori@polimi.it
[c] *Post-Doc Researcher, Politecnico di Milano, Department of Aerospace Science and Technology, Via La Masa, 34, 20156 Milano – Italy*, ivan.troisi@polimi.it
[d] *Associate Professor, Politecnico di Milano, Department of Aerospace Science and Technology, Via La Masa, 34, 20156 Milano – Italy*, antoniomattia.grande@polimi.it
[e] *Full Professor, Politecnico di Milano, Department of Aerospace Science and Technology, Via La Masa, 34, 20156 Milano – Italy*, michelle.lavagna@polimi.it
[f] *Full Professor, Politecnico di Milano, Department of Aerospace Science and Technology, Via La Masa, 34, 20156 Milano – Italy*, giuseppe.sala@polimi.it
* Corresponding Author

Abstract

Utilization of the lunar regolith will have a central role in supporting the exploration of the lunar surface. Numerous technologies are under study these years to exploit the uppermost layer of the lunar surface, among which the extraction of oxygen and water from minerals and additive manufacturing have a pivotal role. At Politecnico di Milano, ongoing research and demonstration efforts are directed towards the low-temperature carbothermal reduction of lunar surface material, employing a two-step process involving carbothermal and methanation reactions. This approach aims to extract water from lunar minerals, demonstrating versatility by accommodating a wide range of possible regolith feedstock compositions. Nevertheless, the optimization of process yield and water production warrants strategic selection of specific minerals. The lunar highlands regolith is composed of iron-rich basalts and iron-poor anorthosite, which may be separated in the dedicated magnetic beneficiation stage with the help of an electromagnet. It was shown that after separation these two fractions can be used more efficiently than the non-refined genuine feedstock. While the iron-rich basalt is not well suited for stereolithography-based 3D printing due to its high absorption in the UV range, it yields a higher oxygen production rate during the carbothermal process, thanks to the lower oxygen bonding energy. On the other hand, it was found that iron-poor anorthosite fraction is a perfect feedstock for ceramic manufacturing via stereolithography-based AM, due to its lower UV absorption and higher melting temperature. Thereby, it was experimentally shown that the introduction of preliminary magnetic beneficiation of lunar regolith may contribute to increasing the oxygen production rate and improving the printability of the regolith via stereolithography-based AM, showcasing a holistic and integrated approach to lunar regolith utilization.

Keywords: ISFR, ISRU, Moon exploration, lunar regolith, additive manufacturing, 3D-printing, Oxygen extraction, Water extraction, Carbothermal reduction.

Acronyms/Abbreviations

AM	Additive Manufacturing
ASI	Italian Space Agency
DSC	Differential Scanning Calorimetry
ISFR	In Situ Fabrication and Repair
ISRU	In Situ Resources Utilization
PoliMi	Politecnico di Milano

1. Introduction

In recent years the interest in sustainable lunar exploration and the utilization of in-situ resources (ISRU) significantly developed, as the leading space agencies and aerospace companies are focusing more and more on returning humanity to the Moon. In this regard, the lunar regolith presents a valuable in-situ resource that could significantly reduce the need for Earth-launched supplies and enable long-term lunar presence.

Another important aspect of ISRU is the utilization of lunar regolith for additive manufacturing on the lunar surface. This approach may help to enable the production of various structures, components, and tools directly on the lunar surface, significantly improving the redundancy of the future lunar settlement. Possible fields of application include the construction of habitats, radiation

shielding, landing pads, and infrastructure elements. The prospects of manufacturing precise on-demand items and spare parts from lunar regolith ceramics are particularly promising: this capability would allow lunar missions to produce replacement components for life support systems, scientific instruments, and exploration vehicles as needed, enhancing mission flexibility and reducing reliance on Earth-based supply chains.

Due to the oxygen abundance in the lunar regolith, as its minerals are composed of ~45% oxygen, different methods that allow its extraction are under study [1]. Among the different techniques, the most promising ones are the carbothermal reduction, conducted by keeping the regolith in a solid state or melted, the FFC molten salt electrolysis, and the molten regolith electrolysis. In recent years, Politecnico di Milano (PoliMi) investigated the solid-state carbothermal reduction from the theoretical point of view [2] and used a demonstrator plant built under an ESA contract in collaboration with OHB. [3] A Phase A/B study on a scaled version of the plant is currently ongoing with the Italian Space Agency (ASI). [4] Summarising the key elements of the process, a carbothermal reactor hosts the regolith, that reacts with H_2 and CH_4 at 1100°C. The products of the reaction, CO and CO_2, together with the remaining reactants, are passed to a catalytic methanation stage and converted into H_2O and CH_4 again, with abundant H_2 still in the flux. The water vapor is condensed in a dedicated separation unit, while the gases can be recycled to close the loop. The lack of fine beneficiation steps and constraints on the landing location, the relatively easy operability, the low temperatures involved, and the self-sustainability of the process for long durations, make this process a suitable candidate in the ISRU panorama.

Even if the proposed process shows good adaptability to various regolith compositions, optimizing regolith feedstock may help to increase O_2/water production yield. The lunar highlands regolith, which covers most of the perspective lunar base sites on the lunar South Pole, is composed of iron-rich basalts and iron-poor anorthosite, presenting an opportunity for refinement through magnetic beneficiation. It was previously found that the basalt-rich mare regolith is less suitable for stereolithography-based 3D printing than the basalt-poor highland regolith [5], due to its high absorption in UV-range, restricting the printability of mare regolith-infilled slurries. This leads to the idea of magnetic beneficiation of regolith: separation of the basalt contained in highland regolith may help to improve its printability even further, decreasing the printing times and improving the mechanical properties of final parts. On the other hand, it can be proven that iron-rich minerals (basalt and ilmenite), contained in lunar regolith, exhibit superior oxygen production rates in the carbothermal process, compared to the iron-free anorthite counterpart. In [2], the most reactive species are identified, with the Fe oxides being among the easiest to reduce.

This paper will discuss the experimental and theoretical findings that demonstrate the effect of separating these regolith fractions using permanent magnets, and how this separation can lead to more efficient utilization of the regolith for both oxygen

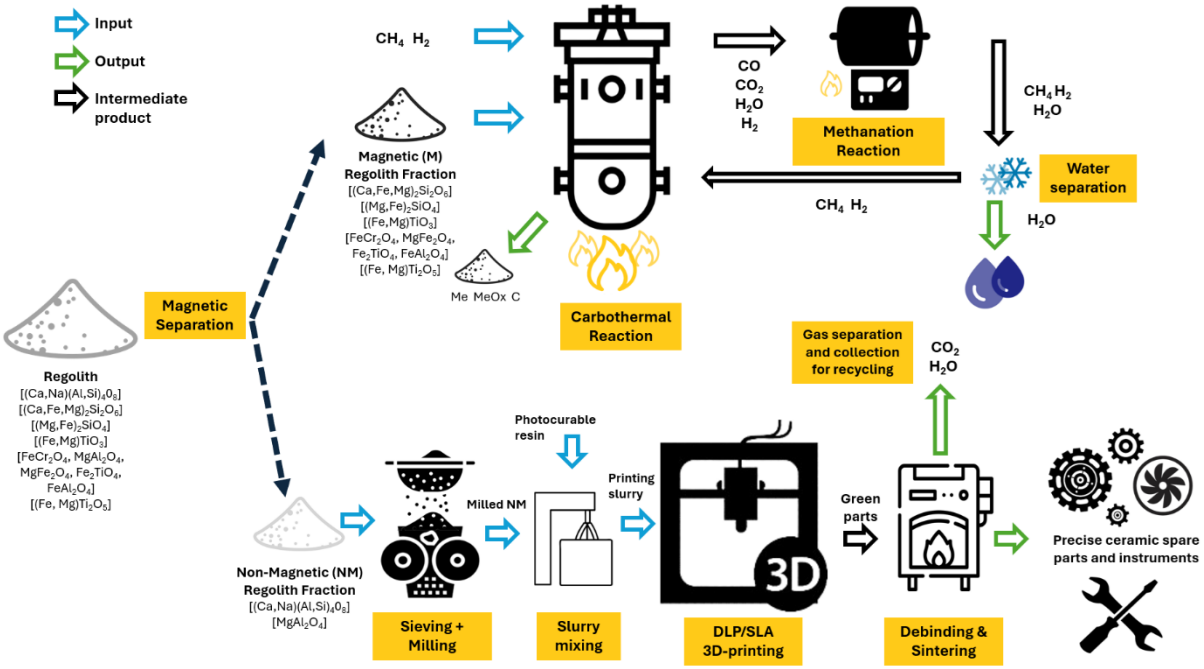

Figure 1 Magnetic separation + Carbothermal Process and Additive Manufacturing Process

Table 1 The six powder samples after milling.

Sample name	Description	Anorthite content [wt.%]	Basalt + Ilmenite content [wt.%]
LHS-25	Milled unrefined highland regolith	75	25
LMS-75	Milled unrefined mare regolith	25	75
NM-1	Milled non-magnetic fraction of LHS-1	99	<1
M-99	Milled magnetic fraction of LHS-1	<1	99
NM-2.5	Milled NM(97.5%)/M(2.5%) mixture	97.5	2.5
NM-5	Milled NM (95%)/ M(5%) mixture	95	5

production and additive manufacturing, eventually helping to harvest the full potential of lunar resources.

The joint process is visually summarized in Figure 1.

2. Material and methods

2.1 Experimental tests on magnetic separation and Additive Manufacturing

For the tests, the Lunar Highlands (LHS-1) and Lunar Mare (LMS-1) simulants were purchased from the SRT (former University of Central Florida's Exolith lab [6], [7]). The LHS-1 simulant accurately mimics the chemical and mineral composition of lunar highlands, composed mainly from anorthite, whereas the LMS-1 simulates basalt-rich lunar mare soils. Both simulants contain mineral particles ranging in size from 10 to 200 µm, which correlates with data on original Apollo samples [8].

2.2 Investigation of the regolith composition impact on the carbothermal process

The theoretical investigation conducted to predict the effects on the process varying the regolith composition is conducted with the aid of different tools and previous experiments. Two main effects are studied:

- Impact on the yield of the carbothermal process.
- Impact on the process temperature.

Indeed, the former is important to optimize the product of the reaction. The latter, instead, is important to maintain a solid feedstock, still in sandy form, and easy the removal of the reacted material at the end of the process.

2.2.1 Regolith composition impact on the yield

The investigation yield of the carbothermal reaction varying the soil composition is conducted with the aid of two pieces of information. The first comes from the tool developed in [2]: according to the Gibbs Free Energy trends of each species, the species that react are identified. The second, instead, takes the data obtained during the experimental campaign conducted at PoliMi on the plant described in [3]. The baseline is one of the experiments from the PoliMi experimental campaign: during this test, 4.9 g of oxygen (5.5 g of water) were produced in about 44 h of process from 50 g of NU-LHT-2M lunar simulant (highland type). They correspond to a yield of 21.9% of oxygen produced over the oxygen available in the initial batch of simulant. The water extracted and its yield can be retrieved by molar considerations by converting the extracted oxygen. The choice is to use oxygen as it is directly comparable with the oxygen present in the minerals.

The expected maximum yield obtainable from NU-LHT-2M is evaluated considering that the species that can react from a thermodynamic point of view can fully react. With the hypothesis that all the species contribute at the same rate to the total production, a proportion is made between the yield obtained in the laboratory and the maximum expected one. The evaluation is performed on three simulants, NU-LHT-2M [10], LHS-1 [6], LMS-1 [7], and five different minerals, Anorthosite, Basalt, Bronzite, Ilmenite, Olivine, the constituents [9] of the LHS-1 and LMS-1 simulants [8].

2.2.2 Regolith composition impact on the process temperature

Regolith is composed of different minerals, as stated in the previous paragraph, each of them has a different melting point. The knowledge of the temperature at which the regolith starts to melt is important not only from a gas-dynamic point of view but also in the optic of the exhaust removal. Indeed, in the first case, the melt prevents the gas from flowing uniformly and with no effort with respect to the initial sandy state. In the second case, the interaction between the melt and the vessel causes a difficult removal of the exhaust batch, preventing the re-utilization of the system.

To understand how the regolith and mineral melting temperature are linked, the findings of the study conducted in [11] by means of DSC on the single minerals are reported to predict the behavior of the magnetically separated species.

3. Experimental tests

LHS-1M, LMS-1NM, original LHS-1 and LMS-1 and two additional powder mixtures (95 wt.% NM 5wt% M and 97.5 wt.% NM- 2.5 wt.%) were independently ground with a planetary mill using yttria-stabilized

zirconia (YSZ) milling jars and 2 mm YSZ balls in the presence of isopropyl alcohol (IPA). The m_{IPA}: m_{powder} ratio was 1.5:1, while m_{balls}: m_{powder} ratio was 5:1. The rotation speed of the mill was set to 250 rpm. Milling was performed for 120 min. After milling, IPA was evaporated from the samples in an oven at 60 °C for 24

h. The dried powders were collected for further testing. Table 1 describes six resulting powder samples.

Figure 2 Magnetic LHS-1M powder (left), non-magnetic LHS-1NM powder (right).

To test the photopolymerization response of the beneficiated lunar regolith, lunar simulant-infilled photocurable resins were prepared. The lunar simulant-infilled resins consisted of the above-described milled powders, di-acrylate-based resin, and a suitable phenyl ketone photoinitiator. The powder ratio in the paste was 70 wt.%. Photopolymerization testing was performed using, featuring a 405 nm UV projection system. Square 1x1 cm areas were processed with UV curing of the slurries for 2,5,10,15,30,60 and 120 seconds of exposure. The thickness of the polymerized single-layered samples was measured with Interapid GA thickness gauge (Interapid, Switzerland).

After determining optimal slurry composition, vat-polymerization AM was performed using a Mars 4 DLP-based 3D printer (ELEGOO). STL models of the parts were prepared using Autodesk Fusion CAD software. The layer thickness was set to 20 µm for the printing to achieve the finest resolution and better layer adhesion. The exposure time for curing one layer was set to 15-60s, according to the photo-polymerization depth previously achieved for similar regolith-containing slurries [12]. After each layer was UV-cured, the building platform was raised by 10 mm, allowing a new portion of the slurry to flow under the photopolymerized layer. The manufactured green parts were heat-treated at 1250°C to 1300°C, depending on the in-filling powder's composition.

4. Results and discussion

4.1 AM results

As it was anticipated, a non-magnetic fraction of lunar regolith, mostly composed of anorthite showed much better photopolymerization performance: thanks to the less significant absorption in the UV range, slurries containing less basalt in infilling powder showed higher polymerization depths.

First tests were conducted with a more powerful UV lamp, with an energy output of 40 mW/cm2 at 405 nm wavelength, which helped us to test the darker fractions of lunar regolith, including the magnetic fraction of LHS and LMS powder. To visualize the results we have plotted the achieved thickness of the single polymerized layers, produced from the slurries, containing different regolith species under varying exposure time under UV irradiation. The results are shown in Figure 3.

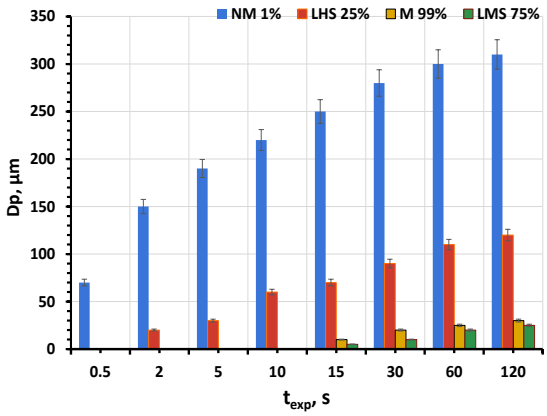

Figure 3 Influence of slurry composition on its photopolymerization performance at various exposure times

Figure 3 shows the dramatic difference in performance for the various types of lunar regolith-containing slurries. It was already shown, how mare regolith-containing slurries underperform in Stereolithography-based AM, compared to highland regolith-based slurries [12], however when compared next to the magnetically beneficiated NM fraction, containing only the trace amounts of basalt, this difference becomes even more significant.

While it takes less than a 1 second to obtain a 50 µm-thick photopolymerized layer, when using an NM slurry, it will take 15 seconds just to get any signs of polymerization from the slurries, infilled with milled lunar mare simulant (LMS) and magnetic (basalt-rich) fraction of LHS.

To further explore more subtle effects of basalt content in the regolith-infilled slurry and to test the beneficiated regolith as a feedstock for an actual DLP-printing machine, we have conducted a similar test, using a DLP printer's UV projection system as a light source (3.7 mW/cm^2 at 405 nm). Figure 4 shows the achieved polymerization depth values for the four different slurries, containing from 1 to 25% of basalt.

Results show that even 2,5% of basalt content is enough to reduce the slurry's performance at photopolymerization significantly (by ~25%).

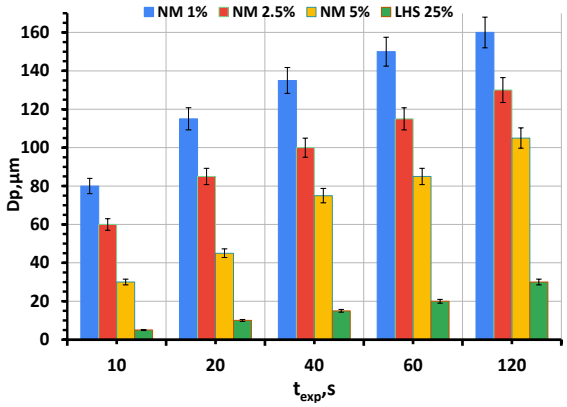

Figure 4 Influence of basal content (1-25 wt.%) on photopolymerization depth of produced single layers

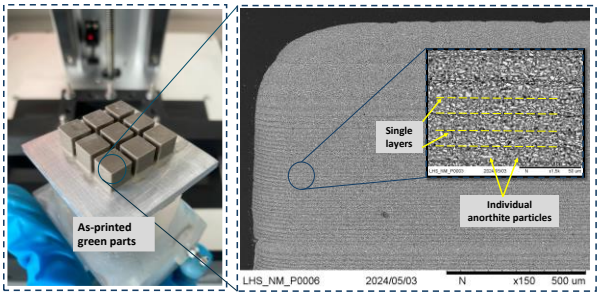

Figure 5 DLP-printed green parts and their microstructure as seen on the SEM

In this regard, we have selected the NM-1 fully beneficiated powder for the actual 3D printing runs. In contrast to the 60 seconds typically required for proper inter-layer bonding during DLP printing with original highland regolith slurries [12], only 10 seconds were needed to achieve well-bonded green parts, using LHS-NM feedstock. With further optimization of the slurry composition, this time could be reduced even further.

The NM green parts produced exhibited a smooth surface finish, strong interlayer adhesion, and good structural integrity. Figure 5 presents the resulting green parts alongside their SEM images.

The SEM images reveal distinct 20 µm layers with excellent inter-layer adhesion. The structure is free of cracks and has a smooth surface with only a few minor defects. Thicker initial layers, seen on the top side of the part, were polymerized with longer exposure times to ensure strong adhesion to the building platform.

The printed green parts were subjected to debinding at 600ºC, followed by sintering at 1250ºC. A higher sintering temperature was chosen compared to our previous study [12], which identified the optimal temperature for sintering highland regolith. This adjustment was made because the NM feedstock contains nearly pure anorthite, which has a significantly higher melting point than the anorthite-basalt mixture in the original highland regolith.

A preliminary 3-point bending test of produced bar-shaped ceramic parts showed a mean ultimate flexural strength of **120±5 MPa.** The produced parts' relative density was measured to be **94%**.

After the first printing trials with simple geometries, we have successfully managed to 3D-print complex lattice parts (Figure 6) as a proof-of-concept of using NM-feedstock. [13]

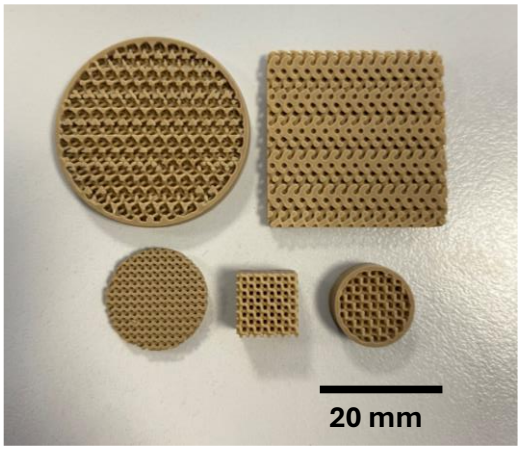

Figure 6 The sintered NM ceramic parts with complex lattice structures

4.2 Composition impact on the carbothermal process: results

4.2.1 Impact on the yield of the process

The first step is the definition of the species that can undergo a carbothermal reduction ($MeO+C \rightarrow CO+Me$ or $MeO+CH_4 \rightarrow CO+2H_2$, with Me a generic species of the oxides present in the lunar minerals) from the thermodynamic point of view. It uses the tool developed in [6], that uses Gibbs' Free energy to evaluate whether a reaction is thermodynamically favored or not. The species that are found to be reactive are SiO_2, TiO_2, Cr_2O_3, FeO, MnO, Na_2O, K_2O, and P_2O_5, while Al_2O_3, MgO and CaO do not react in the 1000-1100°C temperature range.

The second step, instead, follows the indication provided in Section 2.2.1. The results are reported in Table 2 and Table 3.

With the hypothesis that all the species contribute at the same rate to the total production, a proportion is made between the yield obtained in the laboratory on NU-LHT-2M and the maximum expected one: the result is that for 44 h 38.65% of the value is obtained. Therefore,

Table 2 Lunar simulants: contribution of the oxides to the total yield according to the results obtained in DM-P-15, with the assumption that all the reactive oxides react at the same rate. Results for 44h (DM-P-15 duration) over a 50g batch with DM-P-15 alternations are indicated.

Simulant →	**NU-LHT-2M**		**LHS-1**		**LMS-1**	
Species ↓	Composition [wt%]	O_2 produced (44h) [g]	Composition [wt%]	O_2 produced (44h) [g]	Composition [wt%]	O_2 produced (44h) [g]
SiO2	45.09	4.641	49.12	5.055	48.22	4.963
TiO2	0.56	0.043	0.63	0.049	2.7	0.209
Al2O3	27.18	0	26.29	0	12.4	0
Cr2O3	0.11	0.007				
FeO	5.18	0.223	3.2	0.138	8.79	0.378
MnO	0.065	0.003	0.06	0.003	0.06	0.003
MgO	5.84	0	2.86	0	15.97	0
CaO	15.79	0	13.52	0	7.65	0
Na2O	0.47	0.023	2.55	0.127	1.73	0.086
K2O	0.11	0.004	0.34	0.011	0.42	0.014
P2O5	0.12	0.013	0.17	0.019	0.23	0.025
Tot (44h)	100.515	4.957	98.74	5.401	98.17	5.678
Yield O2/O2 (44h) [%]		21.9		23.9		26.0

Table 3 Minerals: contribution of the oxides to the total yield according to the results obtained in DM-P-15, with the assumption that all the reactive oxides react at the same rate. Results for 44h (DM-P-15 duration) over a 50g batch with DM-P-15 alternations are indicated.

Mineral →	**Anorthosite**		**Basalt**		**Bronzite**		**Ilmenite**		**Olivine**	
Species ↓	Composition [wt%]	O2 produced (44h) [g]	Composition [wt%]	O2 produced (44h) [g]	Composition [wt%]	O2 produced (44h) [g]	Composition [wt%]	O2 produced (44h) [g]	Composition [wt%]	O2 produced (44h) [g]
SiO2	49.3	5.074	47.71	4.910	45	4.631	0.4	0.041	39.6	4.076
TiO2	0.1	0.008	1.59	0.123	0.3	0.023	65.7	5.087		0.000
Al2O3	29.4	0	15.02	0	3.3	0	1.7	0	0.8	0
Cr2O3					0.7	0.043	0.1	0.006	0.5	0.031
FeO	0.7	0.030	10.79	0.464	16.5	0.710	26.9	1.158	12.1	0.521
MnO			0.19	0.008	0.3	0.013	1.2	0.052	0.2	0.009
MgO			9.39	0	27.5	0	2.7	0	44.3	0
CaO	19	0	9.9	0	4.8	0	0.2	0	0.4	0
Na2O			2.7	0.135						
K2O	0.3	0.010	0.82	0.027	0.1	0.003				
P2O5	1	0.109	0.66	0.072	1.1	0.120	0.8	0.087	1	0.109
Tot (44h)	99.8	5.231	98.77	5.740	99.6	5.544	99.7	6.432	98.9	4.745
Yield O2/O2 (44h) [%]		22.6		26.5		26.1		36.5		22.3

the same evaluation done for NU-LHT-2M is performed with the mineral constituents using these values to find the expected values after that reaction time. The LHS-1 and LMS-1 minerals are simulated as well to see the differences with respect to the NU-LHT-2M. The magnetically separated simulants LHS-1NM, LHS-1M, LMS-1NM, and LMS-1M, instead, are constituted mainly from anorthosite (LHS-1NM, LMS-1-NM), and the other minerals are included in LHS-1M and LMS-1M (basalt, ilmenite, bronzite, olivine). Olivine can be magnetically separated or not according to the Fe content: for the current evaluations, it is considered separable, however further studies on the composition are planned.

The first observation is that the NU-LHT-2M simulant has a lower oxygen content with respect to LHS-1 and LMS-1: this means that the results obtained with the single minerals in terms of oxygen produced can not be directly compared with the simulant used so far.

Therefore, it can be better to use directly the LHS-1 and LMS-1 for the comparison. Indeed, making a weighted average of the water produced by the single species using the composition of the simulant, in Table 4

Table 4 Magnetic separation of the species in the LHS-1 and LMS-1 simulants. Composition by mineral.

	LHS-1 Percentage of mineral [%]	LHS-1NM Percentage of mineral (on the right, normalized) [%]		LHS-1M Percentage of mineral (on the right, normalized) [%]		LMS-1 Percentage of mineral [%]	LMS-1NM Percentage of mineral (on the right, normalized) [%]		LMS-1M Percentage of mineral (on the right, normalized) [%]	
Anorthosite	74.4	74.4	100			19.8	19.8	100		
Basalt	24.1			24.1	96.4	32			32	39.6
Bronzite	0.3			0.3	1.2	32.8			32.8	40.9
Ilmenite	0.4			0.4	1.6	4.3			4.3	5.4
Olivine	0.2			0.2	0.8	11.1			11.1	13.8
Tot	99.4		100		100	100		100		100

it emerges that the average is closer to these two simulants than on the NU-LHT-2M one. However, it appears evident that the choice of a highland with respect to a maria soil does not impact consistently the final output, confirming the independence of the carbothermal method from the landing site.

Looking at the oxygen produced by the minerals, it emerges that the value is quite close among all the species, therefore a precise utilization of the laboratory plant components is needed to reduce possible deviations. During the heating phase, only inert shall be used to avoid water production during this phase.

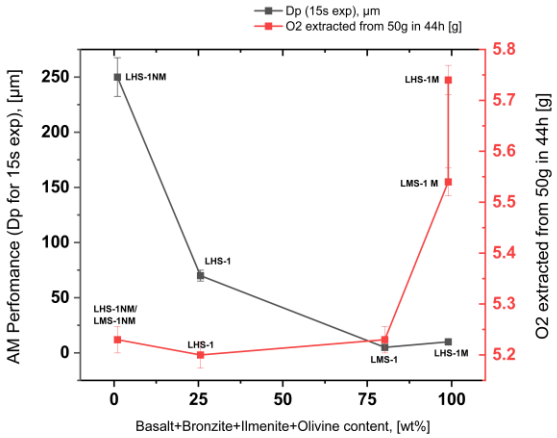

Figure 7 Oxygen extraction with Carbothermal process and Additive Manufacturing performance.

Tests are planned on the different simulants, minerals, and magnetically separated species. These tests are useful to confirm not only these results coming from the thermodynamics, but also from the kinetics, assessing if there are species that react faster or differently from the mixture. In particular, the anorthosite has mainly SiO_2 that reacts, so it is interesting to see its reaction "alone" while included in a mineral. Ilmenite, instead, can offer a view of the ferrous and titanium oxides. The other three are mainly constituted by SiO_2 and FeO as reactive from a thermodynamical point of view: it is offered again the possibility to observe the reaction of SiO_2 and FeO. Once the Anorthosite reaction rate is obtained, as well as the one for Ilmenite (considering together FeO and TiO_2), the new expected results can be obtained and compared with the evaluated ones.

Figure 7 summarizes the results of the oxygen yield varying the composition, going from the magnetic part of the simulant to the non-magnetic ones. All the results are evaluated for 50g of simulant. As expected, there are better results in the right most of the plot, in which the ferrous species are more present. The beneficial effect of having the ferrous species is also expected from the chemical kinetic point of view. However, this will be verified in the laboratory with dedicated experiments to evaluate if the extraction time can be lowered maintaining an equal yield.

4.2.2 Impact on the process temperature

The findings of the study conducted in [11], in which a Differential Scanning Calorimetry (DSC) on NU-LHT-2M (highlands-H), OPRL2NT, used as Maria-HighTi simulant (maria-M), and the previously indicated minerals are performed.

- H-M: M melting temperature (~1050°C) lower than H (1150°C). The reaction temperature needs to be tuned according to the landing location to avoid partial melting. A slope change in the DSC for M (~1160°C) and H (~1270°C) suggests the influence of the basalts.
- Anorthosite: Peaks in the 1000-1200°C range.
- Basalt: Initial phase similar to M. Slope change ~1120°C, similar to H and M.
- Bronzite: Steady decrease to 1300°C, melting at the end. Peaks ~1000°C.
- Ilmenite: Melting at 1300°C, related to M. Initial trend similar to bronzite.
- Olivine: Trend similar to bronzite, stable up to 800°C, peaks around 1120°C.

Therefore, the NM-separated regolith, similar to the anorthosite, does not show particular slope changes and can withstand the process temperature, even going up to 1200°C.

Instead of having a mixture of minerals, the M part is more difficult to study, but basalts have a slope change at around 1120°C, so the process temperature of 1100°C is very close to this limit. The indication is to maintain a

safety margin and start to operate with the M-separated regolith at around 1000°C.

These indications will be useful for the tests planned in the short future to confirm the beneficial effect of a separated regolith, even if it is remarked that the process is able to sustain with good yields all the lunar soils.

5. Conclusions

Magnetic beneficiation has been shown to refine the mineral composition of lunar regolith by selectively concentrating the iron-poor anorthite phase, which is more amenable to stereolithography-based AM. This refinement translates directly into improved process parameters, notably reducing the exposure time per layer from 60 seconds to just 5-10 seconds, achieving a tenfold decrease in overall printing time.

This advancement is critical for future lunar operations, where efficiency and resource conservation are paramount. The resulting ceramic parts exhibit high relative density (**94%**) and mechanical properties, as evidenced by significant flexural strength (**120±5 MPa**), thereby meeting the rigorous demands for structural and functional components in a lunar environment.

By demonstrating that magnetic beneficiation can significantly enhance the efficiency and quality of AM processes, this research supports the viability of utilizing in-situ resources for the fabrication of essential components directly on the lunar surface. This approach reduces the reliance on Earth-supplied materials and aligns with the broader objectives of reducing mission costs and expanding the scope of human activities on the Moon.

From the CRB process point of view, instead, it is proven by using the experimental results obtained on a demo plant at PoliMi and a thermodynamical investigation, that the darker magnetic iron-rich fraction of lunar regolith offers better oxygen yield and opens the path for the investigation of the chemical kinetic of this fraction of regolith. Indeed, the abundance of ferrous compounds can reduce the reaction times, being the most reactive species.

Acknowledgements

This research did not receive any specific grant from funding agencies in the public, commercial, or not-for-profit sectors.

References

[1] L. Schlüter, A. Cowley, Review of techniques for In-Situ oxygen extraction on the moon, Planet. Space Sci., Vol. 181, 2020, 104753.

[2] I. Troisi, P. Lunghi, M. Lavagna, Oxygen extraction from lunar dry regolith: Thermodynamic numerical characterization of the carbothermal reduction, Acta Astronaut. 199 (2022) 113–124.

[3] J. Prinetto, A. Colagrossi, A. Dottori, I. Troisi, M. R. Lavagna, Terrestrial demonstrator for a low-temperature carbothermal reduction process on lunar regolith simulant: Design and AIV activities, Planet. Space Sci. 225 (2023) 105618.

[4] I. Troisi, A. Dottori, M. Lavagna, F. Latini, S. Pirrotta, R. Mugnuolo, Advancements in Lunar Resources Utilization for Oxygen Extraction: Analysis and Design of the ORACLE Payload, IAC-24,D4,5,11,x87784, 75th International Astronautical Congress, Milan, Italy, 2024, 14-18 October.

[5] M. Isachenkov, S. Chugunov, A. Smirnov, A. Kholodkova, I. Akhatov, and I. Shishkovsky, "The effect of particle size of highland and mare lunar regolith simulants on their printability in vat polymerisation additive manufacturing," Ceram Int, vol. 48, no. 23, pp. 34713–34719, Dec. 2022, doi: 10.1016/J.CERAMINT.2022.08.060.

[6] U. of C. F. Exolith Labs, "LHS-1 Lunar Highland Simulant spec sheet," 2021.

[7] U. of C. F. Exolith Labs, "LMS-1 Lunar Mare Simulant spec sheet," 2021.

[8] M. Isachenkov *et al.*, "Characterization of novel lunar highland and mare simulants for ISRU research applications," *Icarus*, vol. 376, no. December 2021, p. 114873, 2022, doi: 10.1016/j.icarus.2021.114873.

[9] U. of C. F. Exolith Labs, "Exolith Lunar Simulants Constituent Report," 2023.

[10] NU-LHT-2M, U.S. Geological Survey Material Data Sheet

[11] A. Dottori, I. Troisi, M. R. Lavagna, Francesco Latini, Mineral-specific impact on the low-temperature carbothermal reduction of lunar regolith, European Lunar Symposium, Scotland, United Kingdom, June 16-21, 2024

[12] Isachenkov, M., Grande, A. M., & Sala, G. (2024). Optimizing Lunar Regolith for Vat Polymerization and Sintering: Pre-processing & Mineral Composition Impact. Ceramics International. https://doi.org/10.1016/J.CERAMINT.2024.06.034

[13] M. Isachenkov, R. Pisani, A.M.Grande, G. Sala, Enhancing Additive Manufacturing of Lunar Regolith Ceramics through Magnetic Beneficiation, IAC-24,A3,IP,189,x84077, 75th International Astronautical Congress, Milan, Italy, 2024, 14-18 October.